PLOS ONE

RESEARCH ARTICLE

Biomechanics of subtrochanteric fracture fixation using short cephalomedullary nails: A finite element analysis

Dae-Kyung Kwak[1], Sun-Hee Bang[2], Won-Hyeon Kim [3], Sung-Jae Lee[2], Seunghun Lee[1], Je-Hyun Yoo [1]*

1 Department of Orthopaedic Surgery, Hallym University Sacred Heart Hospital, Hallym University School of Medicine, Anyang, South Korea, 2 Department of Biomedical Engineering, Inje University, Gimhae, South Korea, 3 Department of Mechanical Engineering, Sejong University, Seoul, South Korea

☯ These authors contributed equally to this work.
* oships@hallym.ac.kr

Abstract

A finite element analysis was performed to evaluate the stresses around nails and cortical bones in subtrochanteric (ST) fracture models fixed using short cephalomedullary nails (CMNs). A total 96 finite element models (FEMs) were simulated on a transverse ST fracture at eight levels with three different fracture gaps and two different distal locking screw configurations in both normal and osteoporotic bone. All FEMs were fixed using CMNs 200 mm in length. Two distal locking screws showed a wider safe range than 1 distal screw in both normal and osteoporotic bone at fracture gaps ≤ 3 mm. In normal bone FEMs fixed even with two distal locking screws, peak von Mises stresses (PVMSs) in cortical bone and nail constructs reached or exceeded 90% of the yield strength at fracture levels 50 mm and 0 and 50 mm, respectively, at all fracture gaps. In osteoporotic bone FEMs, PVMSs in cortical bone and nail constructs reached or exceeded 90% of the yield strength at fracture levels 50 mm and 0 and 50 mm, respectively, at a 1-mm fracture gap. However, at fracture gaps ≥ 2 mm, PVMSs in cortical bone reached or exceeded 90% of the yield strength at fracture levels ≥ 35 mm. PVMSs in nail showed the same results as 1-mm fracture gaps. PVMSs increased and safe range reduced, as the fracture gap increased. Short CMNs (200 mm in length) with two distal screws may be considered suitable for the fixation of ST transverse fractures at fracture levels 10 to 40 mm below the lesser trochanter in normal bone and 10 to 30 mm in osteoporotic bone, respectively, under the assumptions of anatomical reduction at fracture gap ≤ 3 mm. However, the fracture gap should be shortened to the minimum to reduce the risk of refracture and fixation failure, especially in osteoporotic fractures.

Introduction

Osteosynthesis of subtrochanteric fractures is challenging due to the displacement of bone fragments by muscle forces. Intense medial compression and lateral tensile forces are concentrated in the fracture region. These deforming forces make it difficult to achieve anatomical

reduction and fixation, often leading to non-union, malunion, and mechanical failures [1,2]. The overall incidence of non-union or delayed union of subtrochanteric fractures and subsequent failure varies from 7% to 20% [3,4].

Cephalomedullary nails (CMNs), due to their biomechanical superiority to extramedullary implants, have been used as the preferred devices for treating subtrochanteric fractures [5,6]. Favorable clinical results have been reported following the treatment of subtrochanteric fractures using CMNs [7,8], and both short and long CMNs are currently used in the management of subtrochanteric fractures. A long CMN has a biomechanical advantage over a short CMN as it provides improved stability due to a longer working length and protects the remnants of the femur shaft below the fracture site [9,10]. Short CMNs have several advantages such as shorter operative and fluoroscopy times, less blood loss, and lower cost than long CMNs [11,12]. Subtrochanteric fractures usually occur in elderly patients, and the incidence of subtrochanteric fractures in osteoporotic elderly patients, including atypical subtrochanteric fractures, is expected to increase in the future [13,14]. It is important to reduce operation time and decrease blood loss during hip fracture surgery in elderly patients with multiple comorbidities and poor physical conditions [15]. Considering these factors, the use of short CMNs would be more advantageous than the use of long CMNs, especially in elderly patients with subtrochanteric fractures. Although CMNs are commonly used for the surgical treatment of subtrochanteric fractures, the indications for the use of short versus long CMNs still remain unclear [11,16,17]. Furthermore, there is little information on appropriate criteria or indications for the usage of short nails in subtrochanteric fractures with various fracture levels and gaps.

Therefore, we conducted this study to investigate the stress in the CMNs and the circumferential cortical bone at various fracture levels and gaps using short nails with two different numbers of distal locking screws in subtrochanteric fracture models and the fracture patterns in which short nails can be used in normal and osteoporotic bones by finite element analysis. Our hypotheses were that 1) short nails can be used limitedly in subtrochanteric fractures; 2) two distal locking screws would have the wider safe range than one distal locking screw; 3) the safe range would be different according to the fracture level and gap, and bone quality.

Materials & methods

Finite element model (FEM)

A three-dimensional femoral FEM, verified in previous literatures, was used in this study [18–20]. Computed tomography (CT)-scanning of a left intact femur was performed at 1.0-mm transverse resolution in 1.0-mm increments. After extracting the outline of each CT slice image through reconstruction using the Mimics (version 21.0, Materialise, Leuven, Belgium) program, it was stacked in three dimensions to obtain the line and surface of the entire femoral shape. Lines and surfaces constructed in three dimensions were corrected for distorted areas and then subjected to a segmentation process to obtain a final three-dimensional femoral shape. The volume of the cortical and cancellous bone was created using this shape, and a femoral FEM was implemented through meshing process. To verify the finite element model, strain was measured by attaching a strain gauge at a total of 20 points on the anterior, posterior, medial, and lateral sides of the model, and compared with the previous study according to the method conducted by Heiner et al. [19]. An osteoporotic FEM was reproduced according to the previously verified method [21]. Kose et al. [21] reported that cortical thickness index (CTI) was significant measurement indicators to represent the osteoporotic bone model. CTI is calculated as the ratio of cortical thickness to bone diameter 10 cm distal to the lesser trochanter. At CTI value less than 0.3, the correlation with osteoporotic bone showed 100% sensitivity and 98% specificity. Accordingly, we reproduced the osteoporotic bone model
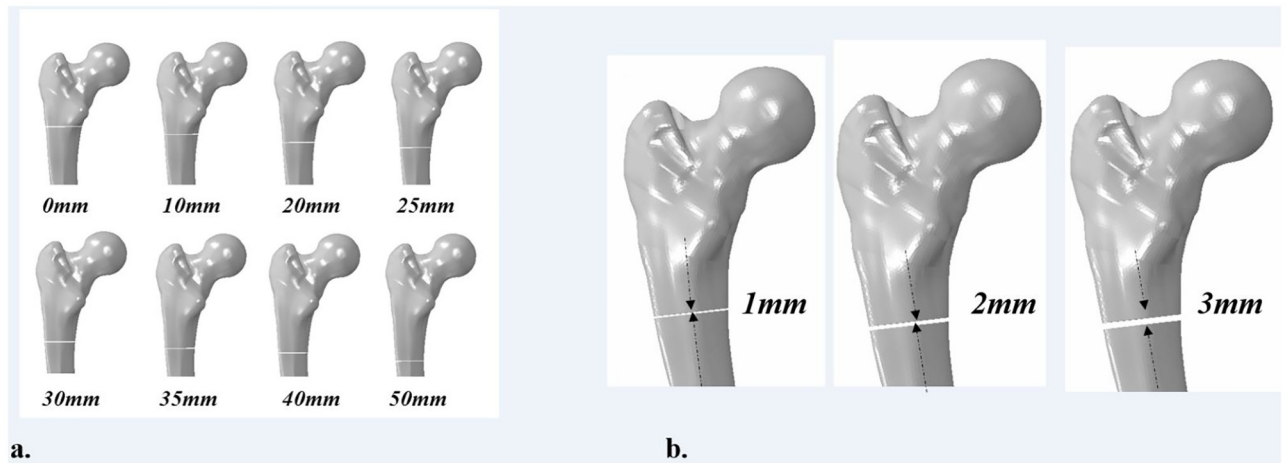
Fig 1. Finite element models with transverse subtrochanteric fracture of different fracture levels.

based on this CTI in this study. To reproduce subtrochanteric fracture models, transverse fracture lines at eight levels in the subtrochanteric region [0, 10, 20, 25, 30, 35, 40, and 50 mm below the lower margin of the lesser trochanter and three different fracture gaps (1, 2, and 3mm) for each of the eight sites were produced on each normal and osteoporotic bone model using ABAQUS (version 6.14, Dassault Systems, Paris, France) (Fig 1).

Short Gamma 3 CMNs (Stryker, Mahwah, NJ, USA), 200 mm in length, 12.0 mm in nail diameter with 125˚ caput-collum-diaphyseal angle, 108-mm lag screw length, and 40-mm distal locking screw length were used in this study. The geometry of all nail configurations was constructed in the intramedullary canal of each FEM using ABAQUS. The lag screw was inserted into the center-to-center position in the femoral head, and the tip-apex distance was set to 22.92 mm in summation of the anterior-posterior and lateral views. Anatomical reduction was assumed in all the models while maintaining the fracture gap. The fracture gap was defined as the longitudinal distance between the two fractured ends at the cortex and the fracture site was assumed free of any bony contact. Short CMNs with two different distal locking screw configurations (1 and 2) were inserted in each FEM using ABAQUS. A total of 96 models were reproduced.

Eight-noded hexahedral elements (C3D8) and four-noded tetrahedral elements (C3D4) were created by using the automatic solid and mesh generation program (ABAQUS/Standard) to build up the mesh of the fractured femur model and the Gamma 3 CMNs. These elements enabled the definition of the different material properties and maintained contact conditions in the fracture plane.

Material properties

The finite element analysis assumed that the bone structure has two different material properties (cortical bone and density-based homogeneous cancellous bone) and isotropic linear properties. To assign cancellous bone properties to the femoral model, the elastic modulus was calculated based on the referred average CT Hounsfield unit (HU) value of 120.8 [22]. The following bone density-HU and elastic modulus-bone density relationships were used [23,24]:

$$\rho = 131000 + 1067 \ HU$$

$$E = 6850 \ \rho^{1.49}$$

Table 1. Material properties applied for the finite element model analysis.

		Elastic Modulus(E) (MPa)	Poisson's ratio(v)
Cortical bone		17000	0.3
Cancellous bone	Normal bone	920	0.2
	Osteoporotic bone	574	0.2
Implant (TI6Al4V)		113800	0.3

where ρ is the apparent density (g/cm^3), and E is the elastic modulus (MPa). The material properties of the femoral cortical bone and nail were referenced from earlier publications (Table 1) [25,26]. Titanium alloy (TI6Al4V) was used for the Gamma 3 CMNs for the purpose of analysis. Different material properties were assigned to different femoral regions.

Boundary and loading conditions

Assuming the 1-leg stance is taken during normal ambulation, a hip joint force (2013.9 N, 300% of the body weight) was loaded on the femoral head, and an abductor muscle force (671.3 N, 100% of the body weight) was applied to the lateral surface of the greater trochanter [27]. Each force was acting at an angle of 20˚ from the vertical line in the frontal plane (Fig 2).

A "tie" contact condition was applied in this study, assuming full constraints between bone and bone, bone and lag screw, and bone and distal locking screw. The general contact condition was applied using a friction coefficient of 0.42 to allow for optimal movement [28].

A total of 96 FEMs were tested using combinations of eight different fracture levels, three different fracture gap sizes, two different bone qualities, and two different distal locking screw configurations. The stresses in the CMNs and the surrounding cortical bone were investigated with emphasis on the fracture level and gap, and the number of distal locking screws in the FEMs and compared to the yield strength. The yield strength values of cortical bones and CMNs were referenced from earlier publications (Cortical bone, 107.9 MPa; TI6A14V, 880 MPa) [29,30].

Validation of the FEM with an implanted CMN

To validate the FEM, we reconstructed a FEM and made an analysis to compare with the published experimental data [31]. In the literature, a mechanical experiment was performed using a composite synthetic bone, and a FEM was reproduced according to the experimental model. The FEM with a fracture level of 0 mm below the lesser trochanter and 1 mm fracture gap, which is the same conditions as in the reference literature, was compared and verified by applying the same load. The results were compared through strain values at the anterior and posterior portion of the lag screw hole, and lateral side of the nail. According to the experiment by Eberle et al. [31], the error rate of the strain difference between the experimental model and the FEM with implanted CMN, was 23%. We compared FEM in this study and the above experimental model as the same method; As a result, the error rate between the FEM in this study and the experimental model in the literature was only 9%. Considering these results, the FEM in this study was satisfactorily validated.

Results

Stress distribution in cortical bone and nail constructs in FEMs with 1-mm fracture gap

Peak von Mises stress (PVMS) in the cortical bone was observed around the distal locking screws in all FEMs regardless of the fracture level, bone quality, and the number of distal locking screws. The PVMS site on the nail constructs tended to move downwards from the
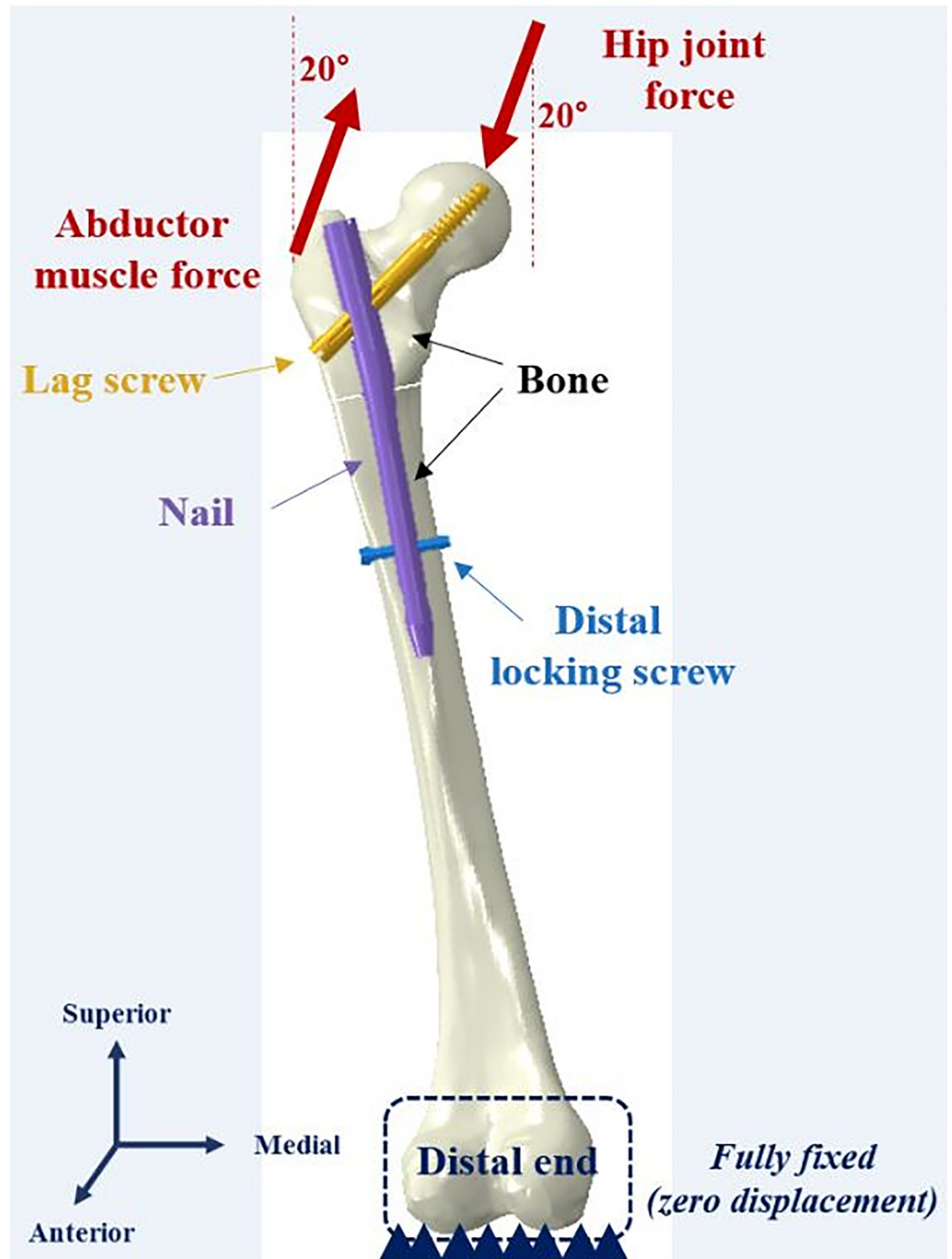
Fig 2. Loading condition of the analysis model; Hip joint force (FH), 2013.9 N (body weight X 300%); Abductor muscle force, 671.3 N (body weight X 100%).

junction with the lag screw through the fracture site to the junction with the distal locking screw with decreasing fracture levels.

In normal bone models, PVMSs in cortical bone and nail constructs (nail body and distal locking screw) were greater than the yield strength at only fracture levels 50 mm below the lesser

Fig 3. Stress distribution around the cortical bone and implant of finite element models using 1 (a, b) and 2 (c, d) distal screw fixation in 1 mm fracture gap, osteoporotic bone. The enlarged image portion represents the point at which the peak stress was observed.

trochanter among FEMs fixed with one distal locking screw. Meanwhile, PVMSs in FEMs fixed with two distal locking screws were less th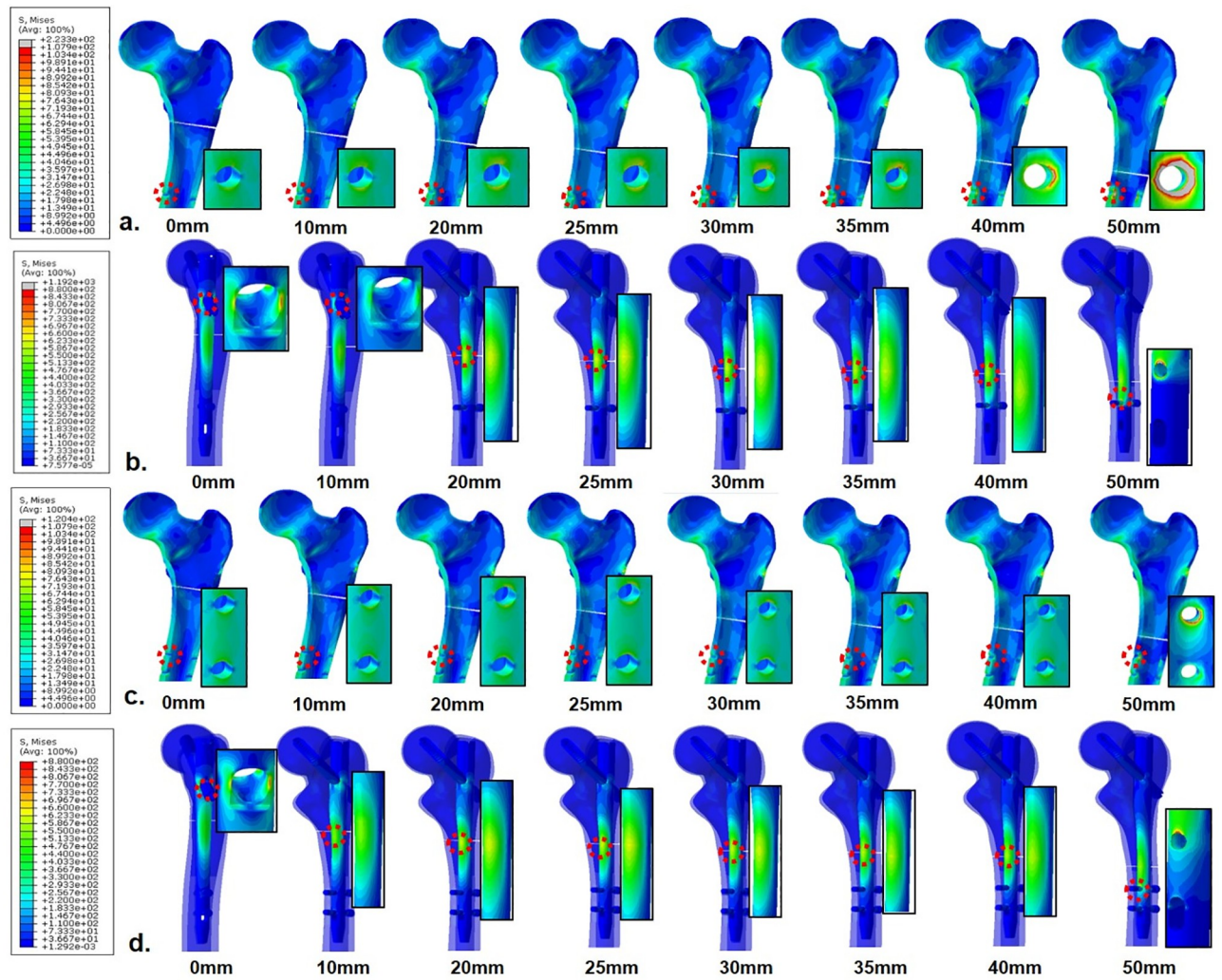an the yield strength at all fracture levels (S1 Fig). In osteoporotic bone models, PVMSs in the cortical bone at fracture levels 50 mm below the lesser trochanter and the junction of the nail body and the lag screw at 0 mm were greater than the yield strength, regardless of the number of distal locking screws. Meanwhile, in FEMs with one distal locking screw, PVMS in the cortical bone was greater than the yield strength at fracture level 40 mm below the lesser trochanter (Fig 3). Therefore, FEMs fixed with two distal locking screws showed a wider safe range in both normal and osteoporotic bone models.

Stress distribution in cortical bone and nail constructs in FEMs with 2-mm fracture gap

In normal bone models, PVMSs in cortical bone and nail constructs (nail body and distal locking screw) were greater than the yield strength at fracture levels $\geq$ 40 mm and 50 mm below the lesser trochanter, respectively, among FEMs fixed with one distal locking screw. Meanwhile,
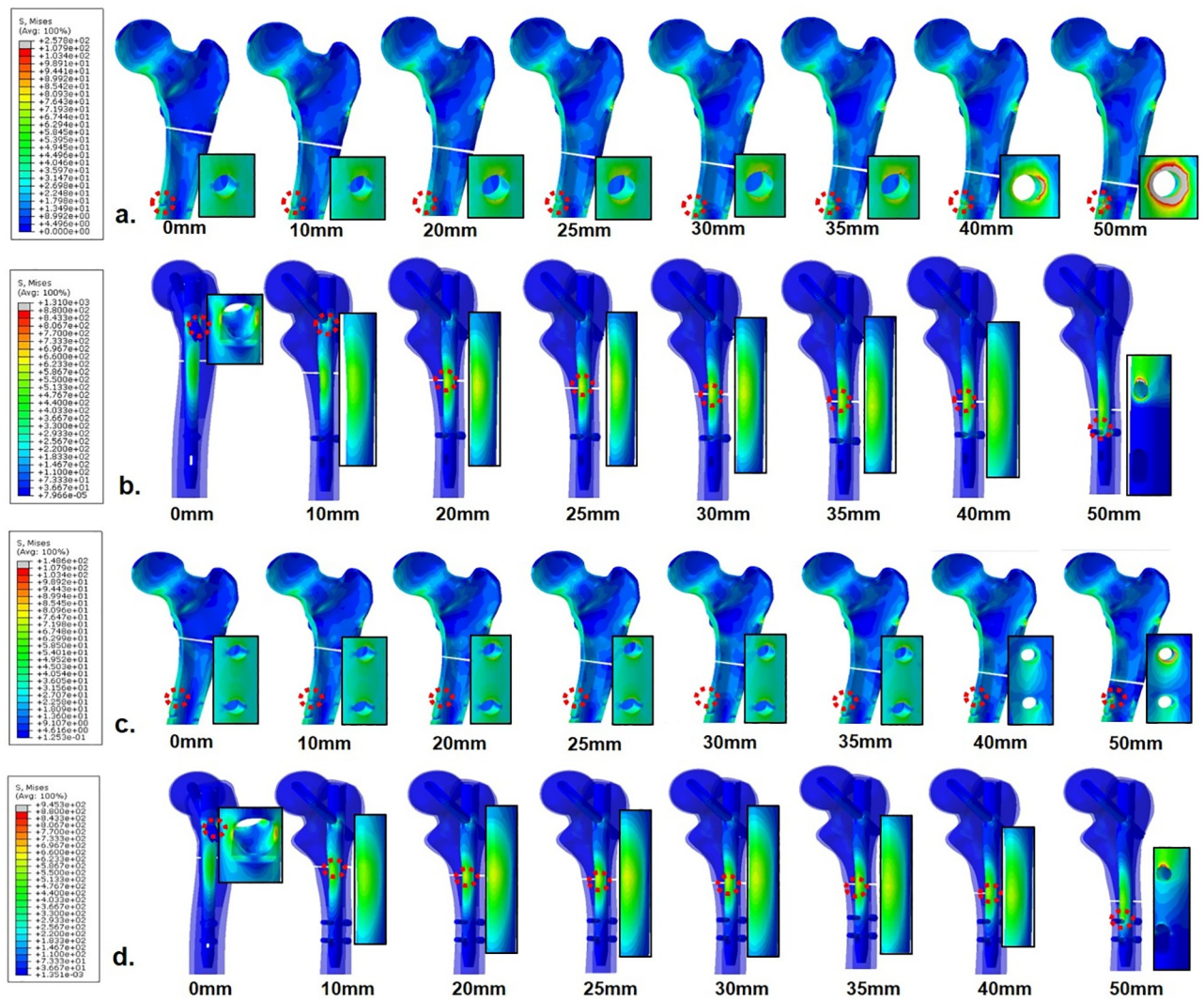
Fig 4. Stress distribution around the cortical bone and implant of finite element models using 1 (a, b) and 2 (c, d) distal screw fixation in 2 mm fracture gap, osteoporotic bone. The enlarged image portion represents the point at which the peak stress was observed.

PVMSs in FEMs fixed with two distal locking screws were greater than the yield strength at only 50 mm below the lesser trochanter (S2 Fig). In osteoporotic bone models, PVMSs in the cortical bone at fracture levels 50 mm below the lesser trochanter and the junction of the nail body and the lag screw at 0 and 50 mm were greater than the yield strength, regardless of the number of distal locking screws. Meanwhile, in FEMs with one distal locking screw, PVMS in the cortical bone was greater than the yield strength at fracture levels ≥ 35 mm below the lesser trochanter (Fig 4). Therefore, FEMs fixed with two distal locking screws showed wider safe ranges in both normal and osteoporotic bone models (Table 2).

Stress distribution in cortical bone and nail constructs in FEMs with 3-mm fracture gap

In normal bone models, PVMSs in the cortical bone and the junction of the nail body and the lag screw at fracture level 50 mms below the lesser trochanter were greater than the yield

Table 2. Summary of Peak von Mises stress in finite element models according to fracture gap.

Fracture gap	Fracture level	Peak Von Mises Stress (MPa)															
		Cortical bone				Nail body				Lag screw				Distal locking screw			
		Normal bone		Osteoporotic bone		Normal bone		Osteoporotic bone		Normal bone		Osteoporotic bone		Normal bone		Osteoporotic bone	
		1 screw	2 screw	1 screw	2 screw	1 screw	2 screw	1 screw	2 screw	1 screw	2 screw	1 screw	2 screw	1 screw	2 screw	1 screw	2 screw
1 mm	0mm	68	65	76	77	789	788	951*	949*	592	592	761	760	109	131	121	146
	10mm	71	67	85	86	542	541	551	548	320	320	411	420	106	128	135	161
	20mm	75	71	93	87	625	625	625	621	204	204	299	299	137	169	188	188
	25mm	78	74	94	89	640	640	643	639	203	203	249	249	157	185	230	190
	30mm	84	79	98	90	614	614	623	622	201	201	208	208	187	190	327	178
	35mm	89	81	104	91	606	605	610	605	199	198	203	202	252	187	405	211
	40mm	98	81	146*	93	582	591	595	593	198	198	205	204	369	225	542	286
	50mm	194*	101	223*	120*	1003*	778	1192*	878	188	190	205	205	992*	581	1245*	642
2 mm	0mm	69	66	76	76	789	788	952*	950*	593	592	761	761	110	131	121	146
	10mm	73	70	89	85	553	552	558	558	320	320	411	411	107	128	139	164
	20mm	74	71	95	86	627	616	626	624	204	205	300	300	140	172	192	189
	25mm	78	74	95	89	638	637	641	640	203	203	250	250	161	186	243	189
	30mm	83	74	102	92	612	612	620	619	201	201	208	209	206	186	317	184
	35mm	96	79	109*	96	604	603	608	607	198	198	203	202	270	185	415	217
	40mm	119*	78	157*	98	591	589	594	591	198	198	204	203	418	252	594	314
	50mm	212*	109*	258*	149*	1106*	843	1310*	945*	187	189	206	205	1082*	626	1308*	687
3 mm	0mm	72	67	81	78	790	789	926*	951*	593	592	762	763	109	131	121	146
	10mm	76	73	87	87	563	563	567	567	321	320	411	411	110	128	144	168
	20mm	79	74	92	88	617	626	633	632	206	205	300	300	144	177	207	190
	25mm	85	74	97	88	638	637	641	640	204	204	250	250	167	187	253	188
	30mm	88	75	111*	90	614	614	619	618	202	202	208	208	220	184	337	184
	35mm	98	78	135*	98	605	604	609	609	198	198	203	202	294	186	442	231
	40mm	124*	79	159*	101	591	598	595	592	197	196	204	204	439	268	641	339
	50mm	238*	129*	273*	162*	1215*	909*	1435*	1009*	185	184	205	205	1176*	670	1374*	609

https://doi.org/10.1371/journal.pone.0253862.t002

strength, regardless of the number of distal locking screws. PVMS in the cortical bone at fracture level 40 mm was also greater than the yield strength among FEMs fixed with 1 distal locking screw (S3 Fig). In osteoporotic bone models, PVMSs in the cortical bone at 50 mm and the junction of the nail body and the lag screw at 0 and 50 mm were greater than the yield strength, regardless of the number of distal locking screws. However, in FEMs with one distal locking screw, PVMS in the cortical bone was greater than the yield strength at fracture levels ≥ 30 mm below the lesser trochanter (Fig 5). Therefore, FEMs fixed with two distal locking screws showed a wider safe range in both normal and osteoporotic bone models. Table 2 shows a summary of PVMS in FEMs according to fracture gap.

Discussion

Several studies have used the finite element method to investigate the biomechanics of subtrochanteric fractures [32–34]. However, our understanding of the optimal management of these fractures are still limited. This study highlighted that the use of a short CMN with two distal locking screws may be a viable option in most transverse subtrochanteric fractures at fracture levels 10 to 40 mm below the lesser trochanter in normal bone and at 10 to 30 mm in osteoporotic bone, under the assumptions of anatomical reduction and fracture gaps ≤ 3 mm.
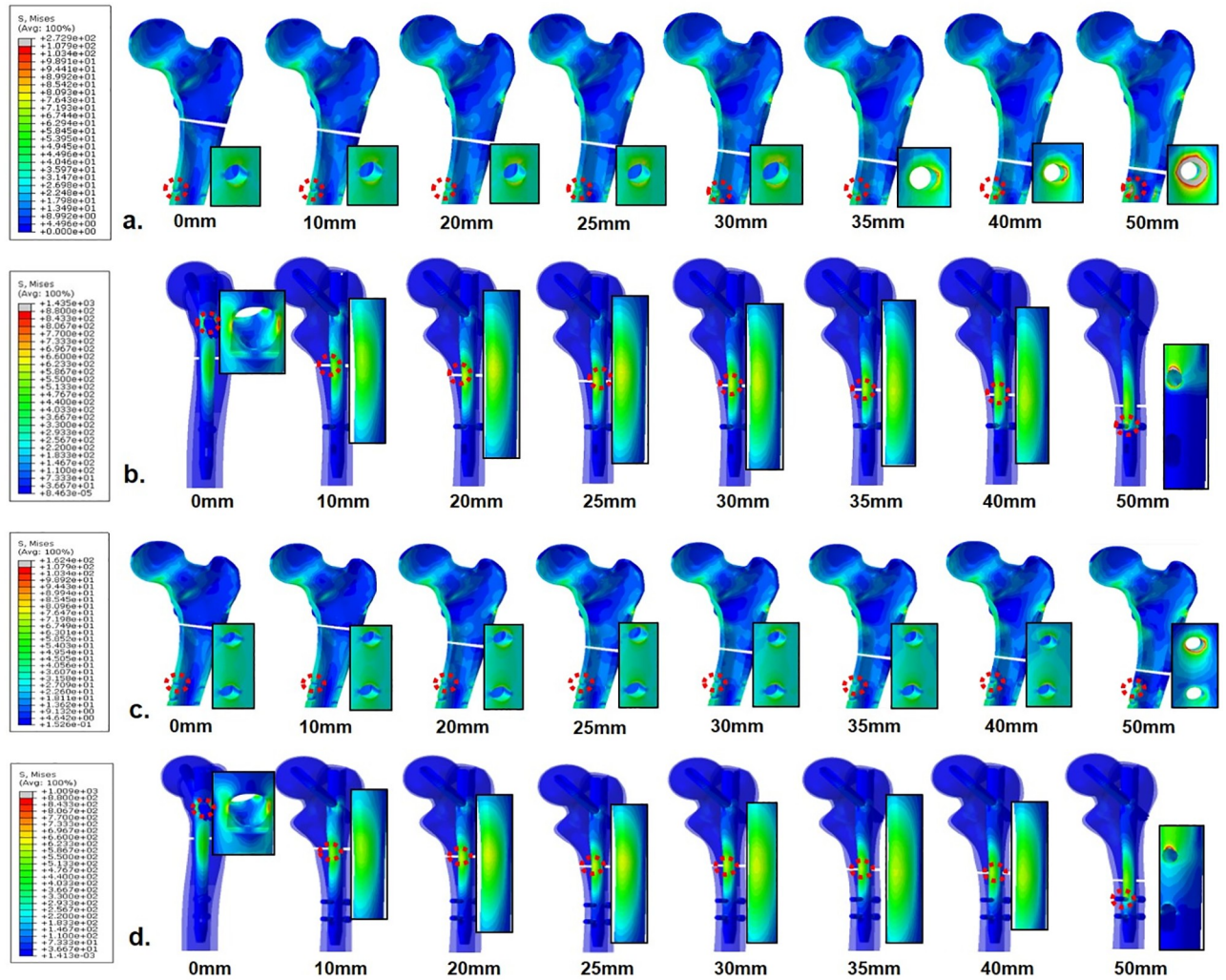
Fig 5. Stress distribution around the cortical bone and implant of finite element models using 1 (a, b) and 2 (c, d) distal screw fixation in 3 mm fracture gap, osteoporotic bone. The enlarged image portion represents the point at which the peak stress was observed.

However, the use of one distal locking screw at fracture gaps ≥ 2 mm reduces the safe range of fracture level for CMNs and would increase the risk of fixation failure or peri-implant fracture. Therefore, short CMNs with one distal locking screw should be avoided in subtrochanteric fractures even with fracture gaps ≤ 3 mm, especially in the osteoporotic bone due to an increase in PVMSs.

CMNs have been widely used in the surgical management of subtrochanteric fractures due to their biomechanical and clinical superiority to extramedullary implants [5,7,8]. Although long nails are generally used for subtrochanteric fractures, short CMNs are also used for high subtrochanteric fractures [35]. However, there are no definite indications or evidences for the use of short CMNs depending on the fracture level and few studies on this issue. The fixation stability in subtrochanteric fractures is of paramount importance because of anatomical geometry of the proximal femur and strong deforming forces in the subtrochanteric region. Several factors including the fracture level, gap, bone quality, nail length, and the number of distal locking screw can affect the fixation stability after nailing in subtrochanteric fractures [36–38].

Therefore, it is difficult to compare and validate the fixation stability clinically under various fixation conditions using short or long nails due to several problems including ethical issues. Besides, there is a lack of evidences on the fixation strength of short CMNs according to fracture level and gap in subtrochanteric fractures and the stresses surrounding those. Therefore, we conducted the current study using FEMs to investigate this issue.

Generally, stress/strain distribution analysis using the finite element methods is widely accepted as a useful technique to evaluate or predict the biomechanical behavior of orthopaedic implants under certain load conditions [33,39,40]. Therefore, this study was conducted to investigate the biomechanics of subtrochanteric fracture fixation using short CMNs using a finite element analysis. In this analysis, we compared the strengths of bone-implant constructs at various fracture levels and gaps using short CMNs with one or two distal locking screws and finally tried to suggest the fracture levels and fixation methods suitable for their use in transverse subtrochanteric fractures in normal and osteoporotic bone models.

All FEMs in this study showed similar stress distribution at PVMS sites around the cortical bone and nail constructs at corresponding fracture levels, regardless of the fracture gap and the number of distal locking screws. PVMS in the cortical bone around the nail was observed at the distal locking screw hole regardless of the fracture level and gap, number of distal locking screws, and bone quality. These values further increased in FEMs using one distal locking screw, and as the fracture level lowered and the fracture gap increased in both normal and osteoporotic bone models. Subsequently, the safe range of the fracture levels for the use of a short CMNs in subtrochanteric fractures was reduced, at which the PVMSs were less than the yield strength. However, PVMSs on this site in osteoporotic FEMs, even fixed with two distal locking screws, showed relatively high values, corresponding to over about 80% of the yield strength at fracture levels 10 to 40 mm below the lesser trochanter, regardless of the fracture gap. Furthermore, PVMSs at the fracture gap ≥ 2 mm were over approximately 90% of the yield strength at fracture levels 35 and 40 mm. These findings suggest that the distal locking screw hole at the medial or lateral cortex may be a stress-riser, causing peri-implant fracture or fixation failure following subtrochanteric fracture fixation using a short CMNs. Therefore, we believe that two distal locking screws should be used, and the fracture gap should be minimized to ≤ 1 mm as far as possible when using a short CMN within the safe range of subtrochanteric fractures, especially in osteoporotic bone. Besides, more caution should be taken to prevent refracture around the distal locking screw and protected weight-bearing with walking aids should be maintained to reduce this risk till bony union. Likely, we focused on the risk of fixation failure during the early postoperative period until the bone union. Therefore, we did not consider cyclic loading in this study.

Meanwhile, as the fracture level goes down, the PVMS site on the nail body tended to move downwards from the junction of the nail body and the lag screw to the junction of the nail body and the distal locking screw. These findings are similar to the results of earlier studies that reported breakage of the CMNs at three principal nail points (the junction of the nail and the lag screw, the distal locking screw, and the fracture site), especially as the lag screw hole and the distal locking screw hole of the nail body are weak points due to the narrow area of the nail [41–43]. In our results, PVMSs on the junction of the nail body and the lag screw at fracture level 0 mm measured over 90% of the yield strength even in normal bone, regardless of the fracture gap and the number of distal locking screws. Moreover, PVMSs on the junction of the nail body and the distal locking screw at 50-mm fracture levels measured over 90% of the yield strength in FEMs fixed even with two distal locking screws, regardless of the fracture gap and bone quality. Based on these findings, we believe that short CMNs should not be used at fracture levels 0 and 50 mm even with two distal locking screws at a 1-mm fracture gap in both normal and osteoporotic bone. According to previous literature, short CMNs can be used for

high subtrochanteric fractures but may be contraindicated for low subtrochanteric fractures due to short distance between the fracture site and distal locking screws [35]. However, short CMNs may be contraindicated in high subtrochanteric fractures just below the lesser trochanter even with two distal locking screws, regardless of the fracture gap and bone quality, considering our results.

The finite element study did not represent the true *in vivo* fracture fixation condition. Ideally, the inclusion of all muscles, joint reactions, and the presence of fracture callus would reveal the true nature of the *in vivo* mechanical response [44]. However, this is not straightforward, and simplified loading conditions will continue to be used in experiments and provide biomechanical guidance on the fracture fixation. The FEM in this study was validated by comparison with previously published models. Furthermore, we reproduced various models according to the fracture level and gap, the number of the distal locking screws and bone quality. Therefore, we believe that this experimental study suggests the novel evidence related to the usage of short nails in limited conditions of subtrochanteric fractures although this does not provide the absolute criteria for the usage of short nails in the treatment of subtrochanteric fractures.

There are some limitations to this study. First, the complex physiological force components around the proximal femur were simplified as physiologic loading during activities is more complex, and greater loading can occur in real-life situations. However, only axial loading, which simulated the forces of a 1-legged stance, was considered appropriate for this finite element analysis as protected weight-bearing with walking aids after operation is recommended until bony union is obtained. Second, we conducted this study under the linear static condition only so fatigue fracture was not considered in this study. Fatigue fracture can occur with long-term repeated loading after the fixation for the femoral fractures. However, we focused on the risk of fixation failure or refracture during early postoperative period until the bone union in this study. Therefore, we did not consider fatigue fracture requiring long-term cyclic loading. Third, we could not decide the exact interaction between the nail and the bone. Although the friction coefficient of 0.42 was assumed as the general contact, it is difficult to accept this value for perfect reproducibility as it is difficult to decide the precise interaction at the implant-bone interface. Besides, we did not consider the effect of screw-bone interface modelling in the clinical conditions [45]. However, intramedullary nailing simulated in this study may be less affected by the screw-bone interface than plate-screw fixation and all models would be similarly affected under the same contact condition of distal locking screw-bone interface. Finally, our results would be not universally valid for all subtrochanteric fracture types because we aimed at subtrochanteric transverse fractures, which are consistently reproducible. However, we believe that the use of short CMNs in other patterns of subtrochanteric fractures could be decided based on our results; this is because subtrochanteric fracture patterns are varied, and there is insufficient evidence for the use of short CMNs in these fractures.

A major strength of this study is that, to our knowledge, it is the first finite element analysis study to investigate the stress distribution around short CMNs used in the fixation of subtrochanteric fractures at various fracture levels and gaps and to evaluate the fixation strength according to the number of distal locking screws and bone quality. Finally, this finite element analysis study simulated various situations of 96 FEMs of subtrochanteric fractures fixed using short CMNs according to different fracture levels and gaps, bone quality, and the number of distal locking screws. However, large-cohort clinical studies are needed to verify the results of this study and to determine the viability of short CMNs for subtrochanteric fractures as this is an experimental study using finite element analysis.

Conclusions

In the current study, two distal locking screws showed a wider safe range than one distal screw when short CMNs were used in subtrochanteric transverse fractures in both normal and osteo-porotic bone models under the assumptions of anatomical reduction at fracture gaps $\leq$ 3 mm. Short CMNs with two distal locking screws may be considered as a suitable option for the fixation of subtrochanteric transverse fractures at fracture levels 10 to 40 mm below the lesser trochanter in normal bone and at 10 to 30 mm in osteoporotic bone under the same assumptions. However, the fracture gap should be reduced to the minimum to lower the risk of refracture and fixation failure, especially in osteoporotic fractures. Accordingly, we carefully suggest that a short CMN may be considered as an available treatment option for subtrochanteric fractures under these conditions. Finally, we believe that our results provide fundamental basic outputs and relative indications for using short CMNs in subtrochanteric fractures.

Supporting information

S1 Fig. Stress distribution around the cortical bone and implant of finite element models using 1 (a, b) and 2 (c, d) distal screws fixation in 1 mm fracture gap, normal bone. The enlarged image portion represents the point at which the peak stress was observed.
(TIF)

S2 Fig. Stress distribution around the cortical bone and implant of finite element models using 1 (a, b) and 2 (c, d) distal screws fixation in 2 mm fracture gap, normal bone. The enlarged image portion represents the point at which the peak stress was observed.
(TIF)

S3 Fig. Stress distribution around the cortical bone and implant of finite element models using 1 (a, b) and 2 (c, d) distal screws fixation in 3 mm fracture gap, normal bone. The enlarged image portion represents the point at which the peak stress was observed.
(TIF)

Author Contributions

Conceptualization: Dae-Kyung Kwak, Je-Hyun Yoo.

Data curation: Won-Hyeon Kim, Seunghun Lee.

Formal analysis: Sung-Jae Lee.

Investigation: Seunghun Lee.

Methodology: Sun-Hee Bang, Sung-Jae Lee.

Software: Sun-Hee Bang.

Supervision: Je-Hyun Yoo.

Validation: Won-Hyeon Kim.

Writing – original draft: Dae-Kyung Kwak.

Writing – review & editing: Je-Hyun Yoo.

References

1. Bedi A, Toan Le T. Subtrochanteric femur fractures. Orthop Clin North Am. 2004; 35(4):473–83. https://doi.org/10.1016/j.ocl.2004.05.006 PMID: 15363922

2. Broos PL, Reynders P. The use of the unreamed AO femoral intramedullary nail with spiral blade in non-pathologic fractures of the femur: experiences with eighty consecutive cases. J Orthop Trauma. 2002; 16(3):150–4. https://doi.org/10.1097/00005131-200203000-00002 PMID: 11880776

3. Sims SH. Subtrochanteric femur fractures. Orthop Clin North Am. 2002; 33(1):113–26, viii. https://doi.org/10.1016/s0030-5898(03)00075-0 PMID: 11832316

4. Craig NJ, Sivaji C, Maffulli N. Subtrochanteric fractures. A review of treatment options. Bulletin (Hospital for Joint Diseases (New York, NY)). 2001; 60(1):35–46. PMID: 11759576

5. Barquet A, Mayora G, Fregeiro J, Lopez L, Rienzi D, Francescoli L. The treatment of subtrochanteric nonunions with the long gamma nail: twenty-six patients with a minimum 2-year follow-up. J Orthop Trauma. 2004; 18(6):346–53. https://doi.org/10.1097/00005131-200407000-00003 PMID: 15213499

6. Saarenpaa I, Heikkinen T, Jalovaara P. Treatment of subtrochanteric fractures. A comparison of the Gamma nail and the dynamic hip screw: short-term outcome in 58 patients. Int Orthop. 2007; 31(1):65–70. https://doi.org/10.1007/s00264-006-0088-9 PMID: 16633810

7. Hotz TK, Zellweger R, Kach KP. Minimal invasive treatment of proximal femur fractures with the long gamma nail: indication, technique, results. J Trauma. 1999; 47(5):942–5. https://doi.org/10.1097/00005373-199911000-00023 PMID: 10568727

8. Kim KK, Won Y, Smith DH, Lee GS, Lee HY. Clinical Results of Complex Subtrochanteric Femoral Fractures with Long Cephalomedullary Hip Nail. Hip Pelvis. 2017; 29(2):113–9. PMID: 28611962

9. Horwitz DS, Tawari A, Suk M. Nail Length in the Management of Intertrochanteric Fracture of the Femur. J Am Acad Orthop Surg. 2016; 24(6):e50–8. PMID: 27128026

10. Menezes DF, Gamulin A, Noesberger B. Is the proximal femoral nail a suitable implant for treatment of all trochanteric fractures? Clin Orthop Relat Res. 2005; 439:221–7. https://doi.org/10.1097/01.blo.0000176448.00020.fa PMID: 16205163

11. Okcu G, Ozkayin N, Okta C, Topcu I, Aktuglu K. Which implant is better for treating reverse obliquity fractures of the proximal femur: a standard or long nail? Clin Orthop Relat Res. 2013; 471(9):2768–75. https://doi.org/10.1007/s11999-013-2948-0 PMID: 23564362

12. Boone C, Carlberg KN, Koueiter DM, Baker KC, Sadowski J, Wiater PJ, et al. Short versus long intramedullary nails for treatment of intertrochanteric femur fractures (OTA 31-A1 and A2). J Orthop Trauma. 2014; 28(5):e96–e100. https://doi.org/10.1097/BOT.0b013e3182a7131c PMID: 24751609

13. Mattisson L, Bojan A, Enocson A. Epidemiology, treatment and mortality of trochanteric and subtrochanteric hip fractures: data from the Swedish fracture register. BMC musculoskeletal disorders. 2018; 19(1):369. https://doi.org/10.1186/s12891-018-2276-3 PMID: 30314495

14. Cooper C, Campion G, Melton LJ 3rd. Hip fractures in the elderly: a world-wide projection. Osteoporosis international: a journal established as result of cooperation between the European Foundation for Osteoporosis and the National Osteoporosis Foundation of the USA. 1992; 2(6):285–9. https://doi.org/10.1007/BF01623184 PMID: 1421796

15. Engoren M, Mitchell E, Perring P, Sferra J. The effect of erythrocyte blood transfusions on survival after surgery for hip fracture. J Trauma. 2008; 65(6):1411–5. https://doi.org/10.1097/TA.0b013e318157d9f9 PMID: 19077635

16. Barquet A, Francescoli L, Rienzi D, Lopez L. Intertrochanteric-subtrochanteric fractures: treatment with the long Gamma nail. J Orthop Trauma. 2000; 14(5):324–8. https://doi.org/10.1097/00005131-200006000-00003 PMID: 10926238

17. Horner NS, Samuelsson K, Solyom J, Bjorgul K, Ayeni OR, Ostman B. Implant-Related Complications and Mortality After Use of Short or Long Gamma Nail for Intertrochanteric and Subtrochanteric Fractures: A Prospective Study with Minimum 13-Year Follow-up. JB & JS open access. 2017; 2(3):e0026. https://doi.org/10.2106/JBJS.OA.17.00026 PMID: 30229225

18. Kwon GJ JM, Oh JK, Lee SJ Effects of Screw Configuration on Biomechanical Stability during Extra-articular Complex Fracture Fixation of the Distal Femur Treated with Locking Compression Plate. J Biomed Eng Res. 2010; 31(3):199–209.

19. Heiner AD, Brown TD. Structural properties of a new design of composite replicate femurs and tibias. J Biomech. 2001; 34(6):773–81. https://doi.org/10.1016/s0021-9290(01)00015-x PMID: 11470115

20. Cristofolini L, Viceconti M, Cappello A, Toni A. Mechanical validation of whole bone composite femur models. J Biomech. 1996; 29(4):525–35. https://doi.org/10.1016/0021-9290(95)00084-4 PMID: 8964782

21. Kose O, Kilicaslan O, Arik HO, Sarp Ü, Toslak İ, Ucar M, et al. Prediction of Osteoporosis through Radiographic Assessment of Proximal Femoral Morphology and Texture in Elderly; is it Valid and Reliable? Türk Osteoporoz Dergisi. 2015; 21:46–52.

22. Lee S, Chung CK, Oh SH, Park SB. Correlation between Bone Mineral Density Measured by Dual-Energy X-Ray Absorptiometry and Hounsfield Units Measured by Diagnostic CT in Lumbar

Spine. J Korean Neurosurg Soc. 2013; 54(5):384–9. https://doi.org/10.3340/jkns.2013.54.5.384 PMID: 24379944

23. Rho JY, Hobatho MC, Ashman RB. Relations of mechanical properties to density and CT numbers in human bone. Med Eng Phys. 1995; 17(5):347–55. https://doi.org/10.1016/1350-4533(95)97314-f PMID: 7670694

24. Morgan EF, Bayraktar HH, Keaveny TM. Trabecular bone modulus-density relationships depend on anatomic site. J Biomech. 2003; 36(7):897–904. https://doi.org/10.1016/s0021-9290(03)00071-x PMID: 12757797

25. Stoffel K, Dieter U, Stachowiak G, Gachter A, Kuster MS. Biomechanical testing of the LCP—how can stability in locked internal fixators be controlled? Injury. 2003; 34 Suppl 2:B11–9. https://doi.org/10.1016/j.injury.2003.09.021 PMID: 14580982

26. Linde F, Hvid I. The effect of constraint on the mechanical behaviour of trabecular bone specimens. J Biomech. 1989; 22(5):485–90. https://doi.org/10.1016/0021-9290(89)90209-1 PMID: 2777823

27. Taylor M. Finite element analysis of the resurfaced femoral head. Proc Inst Mech Eng H. 2006; 220 (2):289–97. PMID: 16669395

28. Lee PY, Lin KJ, Wei HW, Hu JJ, Chen WC, Tsai CL, et al. Biomechanical effect of different femoral neck blade position on the fixation of intertrochanteric fracture: a finite element analysis. Biomedizinische Technik Biomedical engineering. 2016; 61(3):331–6. https://doi.org/10.1515/bmt-2015-0091 PMID: 26351785

29. Bayraktar HH, Morgan EF, Niebur GL, Morris GE, Wong EK, Keaveny TM. Comparison of the elastic and yield properties of human femoral trabecular and cortical bone tissue. J Biomech. 2004; 37(1):27–35. https://doi.org/10.1016/s0021-9290(03)00257-4 PMID: 14672565

30. Heiney J, Battula S, Njus G, Ruble C, Vrabec G. Biomechanical comparison of three second-generation reconstruction nails in an unstable subtrochanteric femur fracture model. Proc Inst Mech Eng H. 2008; 222(6):959–66. https://doi.org/10.1243/09544119JEIM369 PMID: 18935812

31. Eberle S, Gerber C, von Oldenburg G, Hungerer S, Augat P. Type of hip fracture determines load share in intramedullary osteosynthesis. Clin Orthop Relat Res. 2009; 467(8):1972–80. https://doi.org/10.1007/s11999-009-0800-3 PMID: 19333673

32. Mahaisavariya B, Sitthiseripratip K, Suwanprateep J. Finite element study of the proximal femur with retained trochanteric gamma nail and after removal of nail. Injury. 2006; 37(8):778–85. https://doi.org/10.1016/j.injury.2006.01.019 PMID: 16499913

33. Seral B, Garcia JM, Cegonino J, Doblare M, Seral F. Finite element study of intramedullary osteosynthesis in the treatment of trochanteric fractures of the hip: Gamma and PFN. Injury. 2004; 35(2):130–5. https://doi.org/10.1016/s0020-1383(03)00076-7 PMID: 14736469

34. Wang CJ, Yettram AL, Yao MS, Procter P. Finite element analysis of a Gamma nail within a fractured femur. Med Eng Phys. 1998; 20(9):677–83. https://doi.org/10.1016/s1350-4533(98)00079-4 PMID: 10098612

35. Ongkiehong BF, Leemans R. Proximal femoral nail failure in a subtrochanteric fracture: The importance of fracture to distal locking screw distance. Injury Extra. 2007; 38:445–50.

36. Jang CY, Bang SH, Kim WH, Lee SJ, Lee HM, Kwak DK, et al. Effect of fracture levels on the strength of bone-implant constructs in subtrochanteric fracture models fixed using short cephalomedullary nails: A finite element analysis. Injury. 2019. https://doi.org/10.1016/j.injury.2019.08.014 PMID: 31431331

37. Lundy DW. Subtrochanteric Femoral Fractures. JAAOS—Journal of the American Academy of Orthopaedic Surgeons. 2007; 15(11):663–71. https://doi.org/10.5435/00124635-200711000-00005 PMID: 17989417

38. Bredbenner TL, Snyder SA, Mazloomi FR, Le T, Wilber RG. Subtrochanteric fixation stability depends on discrete fracture surface points. Clin Orthop Relat Res. 2005(432):217–25. https://doi.org/10.1097/01.blo.0000150375.13488.a9 PMID: 15738825

39. Sitthiseripratip K, Van Oosterwyck H, Vander Sloten J, Mahaisavariya B, Bohez EL, Suwanprateep J, et al. Finite element study of trochanteric gamma nail for trochanteric fracture. Med Eng Phys. 2003; 25 (2):99–106. https://doi.org/10.1016/s1350-4533(02)00185-6 PMID: 12538064

40. Eggermont F, Derikx LC, Verdonschot N, van der Geest ICM, de Jong MAA, Snyers A, et al. Can patient-specific finite element models better predict fractures in metastatic bone disease than experienced clinicians?: Towards computational modelling in daily clinical practice. Bone Joint Res. 2018; 7 (6):430–9. https://doi.org/10.1302/2046-3758.76.BJR-2017-0325.R2 PMID: 30034797

41. Zafiropoulos G, Pratt DJ. Fractured Gamma nail. Injury. 1994; 25(5):331–6. https://doi.org/10.1016/0020-1383(94)90248-8 PMID: 8034355

42. van den Brink WA, Janssen IM. Failure of the gamma nail in a highly unstable proximal femur fracture: report of four cases encountered in The Netherlands. J Orthop Trauma. 1995; 9(1):53–6. https://doi.org/10.1097/00005131-199502000-00008 PMID: 7714654

43. von Ruden C, Hungerer S, Augat P, Trapp O, Buhren V, Hierholzer C. Breakage of cephalomedullary nailing in operative treatment of trochanteric and subtrochanteric femoral fractures. Archives of orthopaedic and trauma surgery. 2015; 135(2):179–85. https://doi.org/10.1007/s00402-014-2121-6 PMID: 25466724

44. MacLeod A, Simpson A, Pankaj P. Experimental and numerical investigation into the influence of loading conditions in biomechanical testing of locking plate fracture fixation devices. Bone Joint Res. 2018; 7(1):111–20. https://doi.org/10.1302/2046-3758.71.BJR-2017-0074.R2 PMID: 29363522

45. Moazen M, Mak JH, Jones AC, Jin Z, Wilcox RK, Tsiridis E. Evaluation of a new approach for modelling the screw-bone interface in a locking plate fixation: a corroboration study. Proc Inst Mech Eng H. 2013; 227(7):746–56. https://doi.org/10.1177/0954411913483259 PMID: 23636756